

Preparation and properties of PTFE@TiO₂/epoxy superhydrophobic coating

G. Q. Xu^a, C. Q. Li^{a,*}, F. J. Wang^a, J. F. Ou^a, Z. Y. Xue^a, A. Amirfazli^b

^a*School of Materials Engineering, Jiangsu University of Technology, Changzhou 213001, China*

^b*Department of Mechanical Engineering, York University, Toronto ON M3J 1P3, Canada*

The problem of bacterial adhesion has been a challenge in everyday life and industry for decades. In this paper, polytetrafluoroethylene (PTFE) micropowder, titanium dioxide (TiO₂) nanopowder, ethyl acetate and epoxy resin were sequentially added to a beaker and stirred well, then the nanoparticles were modified using perfluorooctyltriethoxysilane (POTS), and finally superhydrophobic coatings were fabricated on the surface of an aluminium sheet by spraying process. Characterisation was carried out using scanning electron microscopy and contact angle measurement, and the coating wettability, chemical stability and mechanical stability properties were investigated, and finally the coating was tested for antimicrobial properties. The study suggests that the hydrophobicity of the sample was optimal at a contact angle of 163.3° and a rolling angle of 3.2° when the ratio of PTFE micropowder to nano-TiO₂ by mass was 1:4 and the ration between POTS and nanoparticles by mass was 12%. The contact angles were 137.8° and 143.6° after 25 and 32 hours of soaked in an anhydrous solution with a pH of 14 and 1, respectively. Most importantly, it exhibits good antimicrobial properties.

(Received September 17, 2023; Accepted November 21, 2023)

Keywords: Superhydrophobic, PTFE micropowder, Nano-TiO₂, Mechanical durability, Antibacterial

1. Introduction

Biofouling poses many hazards, such as fouling of ships, which reduces speed and increases fuel consumption^[1-4], and microbial adhesion to medical devices and food surfaces, which can easily pose a hazard to human safety^[5-7]. In the last decades, several active and passive antimicrobial surfaces based on antibiotics, toxic materials or superwetting structures have been developed^[8,9]. Inspired by lotus leaves, superhydrophobic materials have excellent water repellency properties with e.g. anticorrosive^[10,11], electronic device protection^[12], ice protection^[13,14], self-cleaning^[15,16], oil-water separation^[17-19], drag reduction^[20,21] and antimicrobial^[22] properties. Superhydrophobic surfaces have great potential to resist microbial

* Corresponding author: cql867345327@163.com

adhesion due to their low contact area with water and antifouling properties^[23-26].

There are two main factors for constructing superhydrophobic surfaces: roughness and low surface energy^[27,28]. Based on these two factors, scientists have investigated a variety of preparation methods: spraying^[29,30], hydrothermal^[31], sol-gel^[32,33], self-assembly techniques^[34], vapour phase deposition^[35,36], electrostatic spinning^[37,38], and etching^[39,40]. In the last decades, nano-oxides are widely used to build superhydrophobic coatings because of their unique and advantageous properties. In this nano titanium dioxide is one of the most widely studied materials, which has low cost, abundant content, and good thermal stability, and most importantly, many studies have reported that nano-TiO₂ has an antimicrobial effect^[41-43]. And PTFE micropowder is widely used in coatings due to its chemical resistance, low friction and high temperature resistance^[44]. Ohko et al.^[45] reports that silicon conduits coated with TiO₂ photocatalyst films have a strong bactericidal effect under ultraviolet irradiation. Zhao et al.^[46] added TiO₂ nanoparticles to the Ni-P coating and found that after ultraviolet irradiation, the surface energy (γ -) of the electron donor of the Ni-P-TiO₂ coating significantly elevated with the increase of TiO₂ substance. They also found that with the increase of the surface energy of the coated electron donor, the number of attached bacteria decreased.

For this reason, in this paper, PTFE @ TiO₂/epoxy composite superhydrophobic surface was produced using a single spraying method. The effects of factors such as the mass ration between PTFE micropowder and titanium dioxide nanoparticles and the mass ration between POTS and nanoparticles on the wettability of the sample was studied. The mechanical and chemical stability of the superhydrophobic coating were investigated, and the coating was tested for antibacterial properties.

2. Experimental

2.1. Experimental material

Epoxy resin (EP, E51) was purchased from Kunshan Jurimax Electronic Materials Co. Curing agent (D230) was purchased from Jinan Guangxun Trading Co. Perfluorooctyltriethoxysilane (POTS, analytically pure) was purchased from urn River Chemical Reagent Co. γ -Aminopropyltriethoxysilane (KH550) was purchased from Nanjing Genesis Chemical Auxiliary Co. Nano TiO₂ (30 nm) was purchased from Xuancheng Jingrui New Material Co. PTFE micropowder (1.6 μ m) was purchased from Dongguan Zhongyuan Plastic Raw Material Co. Escherichia coli (ATCC25922) was purchased from Shanghai Luwei Technology Co. Phosphate buffer solution (PBS) was purchased from Guangzhou Hewei Pharmaceutical Technology Co. LB nutrient agar was purchased from Qingdao Haibo Biotechnology Co.

2.2. Preparation of PTFE@TiO₂/epoxy superhydrophobic composite coatings

Aluminium sheets were used as the substrate for the coating. Firstly, the aluminium sheet (5x5cm) was sanded in different directions with 300 mesh sandpaper, then the sanded aluminium sheet was first cleaned with deionized water, then the aluminium sheet was cleaned with anhydrous ethanol by ultrasonic vibration for 30min to remove the residual impurities, and finally was rinsed with deionized water for 2 times and dried for spare.

Firstly, different mass ratios of nano-TiO₂ and PTFE micropowders (total 3.0 g of nano-TiO₂ and PTFE micropowders), 20.0 g of ethyl acetate, and 0.2 g of KH550 were added into a beaker sequentially, and dispersed by ultrasonic shaking for 20 min, and then stirred by magnetism for 1 h (400 r/min), to obtain the well-dispersed mixed solution. Next, an appropriate amount of POTS was increased to the above solution and then magnetically stirred for 3h (400r/min). Finally, epoxy resin (2.7g) and curing agent (0.9g) were increased to the above solution at a mass ratio of 3:1, and dispersed by ultrasonic vibration for 20min, and then magnetically stirred for 3h (400r/min). The above solution was sprayed onto the surface of the aluminium sheet using a single spraying method (the distance between the adjustable nozzle and the aluminium sheet was maintained at about 15cm, and it was slowly sprayed for 1min at 0.5mPa by Z-word technique, and the spraying speed was about 4cm/s), and then cured for 24h at room temperature after the completion of the spraying process, and then the PTFE@TiO₂/epoxy superhydrophobic surface was produced. As shown in Figure 1.

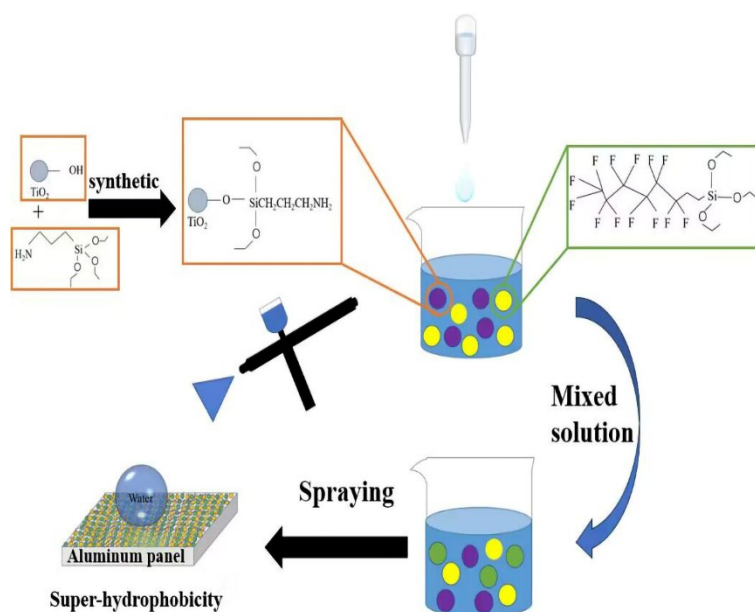


Fig. 1. Diagram of PTFE@TiO₂/epoxy superhydrophobic coating preparation.

2.3. Characterisation of microstructure and wetting properties

The contact and roll angles of the coatings were tested using a contact angle gauge (Krüss, DSA 30) with a quantity of 10 µL of droplets used, by surveying at 5 distinct location of the coating and averaging the values as test values. Thermal field emission scanning electron microscopy (SEM, quantum Q400, FEI, USA) was used to analyse the sample micro-morphology. An energy spectrometer (EDS, GENESIS, EDAX, USA) was used to analyse the elements of the coating. FTIR(Nicolet iS5) was used to analyse the hydrophobically modified nanoparticles.

Abrasion resistance test: steel velvet Abrasion resistance testing machine was used to test the Abrasion resistance of the sample, the weight mass was 100 g, the test speed was 40 cycles per minute, the 1000mesh sandpaper was replaced after 60 cycles, and the contact Angle and

rolling Angle of the sample Abrasion measured every 20 cycles.

Adhesion test: Adhesion test was conducted on the samples with reference to the international standard ISO2409-2013 by drawing scratches on the surface of the samples in the vertical direction with a Baguette knife with a pitch of 2mm, then adhering them to the grid surface with adhesive tape, and finally pulling down the angle slowly at a certain angle.

Antimicrobial test: The antimicrobial test was carried out according to the standard protocol (GB/T 21510-2008, China). A small amount of three-generation slant strain was added to sterile phosphate buffer solution (30.0 ml) under aseptic environment by dipping with an inoculating loop. The coated and control samples were placed in a sterilised petri dish, and 100 μL of *E. coli* (ATCC25922) bacterial solution was taken as a drop on the surface of the samples, and the same samples were covered to the surface of the samples, so that the strains were in full contact with the surface. Then, the petri dish was incubated in a biological incubator (37°C, 3h). The samples were gently washed with sterile phosphate buffer solution to remove residual medium and unattached bacteria. Subsequently, the samples were all immersed in a sampling cup filled with sterile phosphate buffer solution (50.0 mL) and shaken (10 min) to elute the bacteria, which were collected in the sterile phosphate buffer solution. 100 μL of the bacterial solution was spread evenly on nutrient agar plates, and the plates were incubated in a biological incubator at 37°C for 24 h. The number of bacterial colonies in the agar plates was then counted, and three parallel samples were made for each sample and averaged. The antibacterial rate formula is 4-1:

$$R=(B-A)/B \times 100\% \quad (4-1)$$

where R (%) is the antimicrobial rate, A is the number of colonies on the coating and B is the number of colonies on the blank control sample.

3. Results and discussion

3.1. Effect of preparation method

As displayed in Figure 2(a), the rough structure of the material surface has an important influence on the wettability of the material, in this paper, the PTFE micropowder and nano TiO_2 were used to construct the micro and nano rough structure, in the case of the PTFE micropowder alone, the contact angle is 148.2° and the rolling angle is 43.8°, and when using nano- TiO_2 alone, the contact angle is 158.3° and the rolling angle is 4°. When PTFE micropowder was mixed with nano TiO_2 , the contact angle became larger and the rolling angle decreased as the amount of TiO_2 increased and the amount of PTFE decreased; when the mass ration between PTFE micropowder and nano TiO_2 was 1:4, the property of the sample reached the optimum, with a contact angle of 163.3° and a rolling angle of 3.2°. It can be seen that the coating has better hydrophobicity when the ratio of PTFE micropowder to nano TiO_2 mass is 1:4.

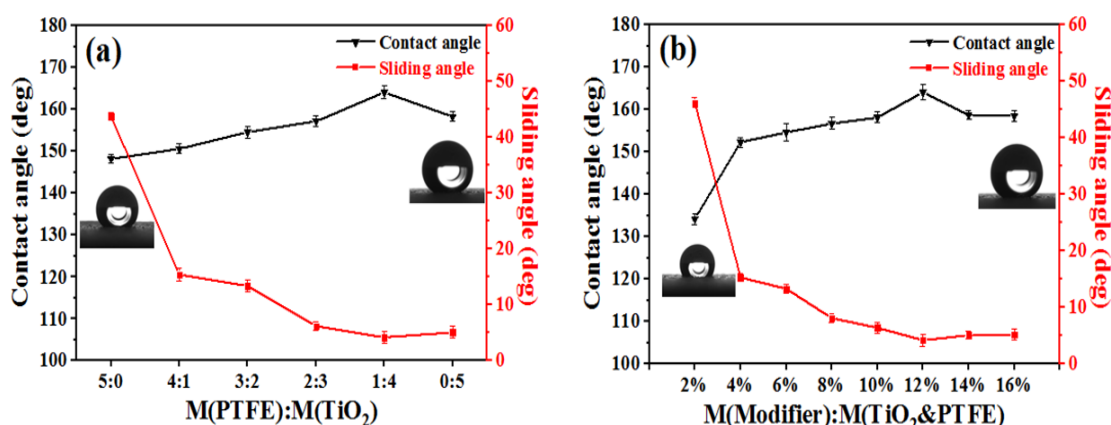


Fig. 2. (a) Effect of mass between PTFE micropowder and nano-TiO₂ on wettability; (b) Effect of mass between POTS and mixed powder on wettability.

Maintaining the mixed powder of PTFE micropowder and TiO₂ nanopowder with 1:4 mass ratio unvarying and other processes unvarying, the effect of mass between POTS and mixed powder on wettability was investigated, and the study suggests that wettability are displayed in Fig. 2(b). There are 2 main factors for constructing superhydrophobic surfaces: one is to construct a lower surface energy, and the other is to construct a surface with a certain roughness. From Fig. 2(b), it is evident that at a POTS to nanoparticle mass ratio of 2%, the contact angle of 134.2° and the rolling angle of 46.2° do not achieve the superhydrophobic effect. As the content of POTS increases, the contact angle rises and the rolling angle falls. At 12% of POTS, the contact angle reaches the highest value of 163.3° and the rolling angle reaches a lower value of 3.2°. As the content of POTS increases, the nanoparticles resist the hydrophilic groups more, the surface energy of the coating is smaller, and the hydrophobicity is stronger. After that, when the content of POTS is increased again, the contact angle and rolling angle basically remain stable, which is due to the fact that it is difficult to continue to reduce the surface energy of the coating after it has reached a certain degree of low. From the economic and practical effect considerations, POTS and nanoparticles mass ratio selected 12% is the best.

3.2. Micro-morphological and chemical composition analysis

Fig. 3(a) and (b) exhibits the SEM pictures of the pure aluminium sheet and the pure epoxy resin coating, respectively, and it can be clearly observed that the surface of the pure aluminium sheet exhibits streak scratches resulting from sanding, and the surface of the pure epoxy resin coating after spraying the pure epoxy resin coating display a homogeneous and smooth morphology without visible micro-nano-structures. Figures 3(c) and (d) show the SEM images of the PTFE@TiO₂/epoxy superhydrophobic coatings, and it can be observed that the prepared PTFE@TiO₂/epoxy superhydrophobic coatings exhibit micro-nano-papillar structures with a much higher surface roughness as compared to pure aluminium flakes and pure epoxy resin coatings. These micro- and nano-scale structures were formed by micro- and nanoparticles combined with epoxy resin aggregates.

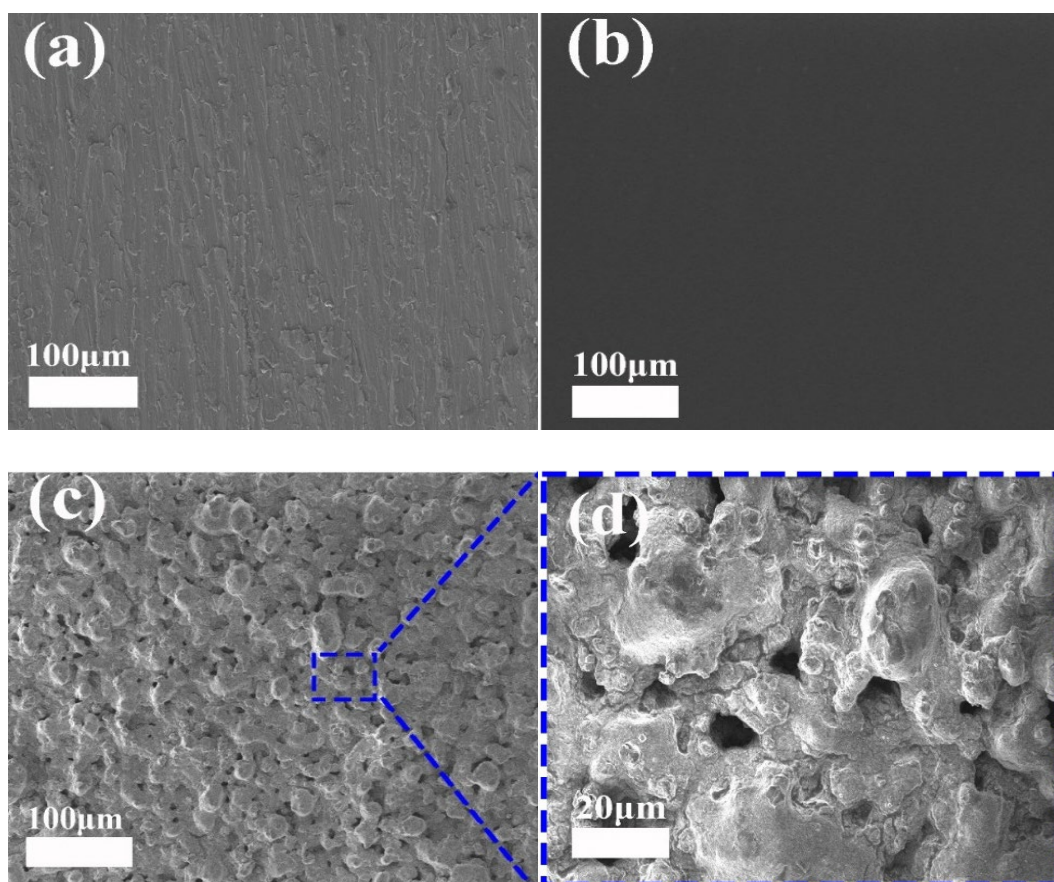


Fig. 3. (a) SEM image of pure aluminium sheet; (b) SEM image of pure epoxy resin coating; (c), (d) SEM image of PTFE@TiO₂/epoxy resin superhydrophobic coating.

The EDS spectra indicate that the coating elements of the coatings comprise C, O, Ti, F, and Si with weight percentages (wt%) of 41.0%, 33.4%, 17.1%, 6.1%, and 2.3%, respectively. As can be seen in Fig. 4, these elements are uniformly distributed on the surface of the coating. The C element is mainly supplied by PTFE micropowder, the Ti and O elements are mainly from nano TiO₂, the F element is mainly supplied by PTFE micropowder and POTS, and the Si element is mainly from the two coupling agents, POTS and KH550. This corresponds to the structure of the PTFE@TiO₂/epoxy superhydrophobic coatings, where the distribution of the three elements C, F and Si are complementary to each other and thus evenly distributed over the entire surface.

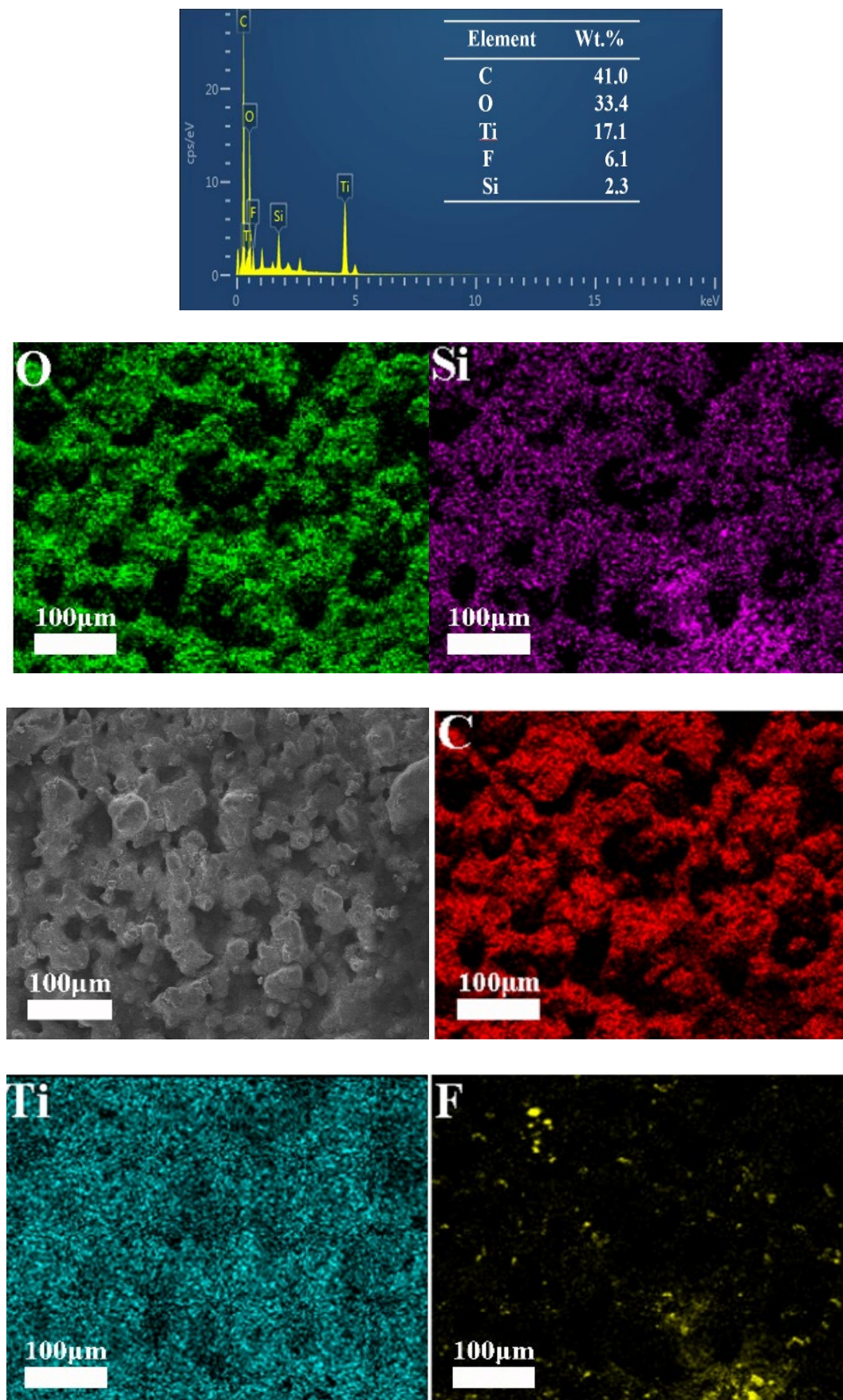


Fig. 4. EDS picture of PTFE@TiO₂/epoxy superhydrophobic coating.

The FTIR of PTFE, TiO₂ and hybrid modified nanoparticles are displayed in Figure 5(a). The telescopic vibrational absorption peak of -OH is at 3349.25 cm⁻¹ in the spectral line, and in Fig. 5(a)^[47], the spectral line b shows a new weak peak at 1047.01 cm⁻¹ in the FT-IR spectrum of modified nanoparticles compared to the spectral lines a and c, which belongs to the KH550 Si-O-Si band^[48]. The peaks at 1243.27, 1144 cm⁻¹ are the stretching vibrational peaks of C-F bonds, which are present in the form of C-F₂ bonds or C-F₃ bonds due to the fluorination of TiO₂ nanoparticles by POTS^[49,50]. The peak at 1144 cm⁻¹ is the Si-O-C bond created by the connection between POTS and TiO₂ nanoparticles^[51]. These results indicate that POTS has been attached to the surface of TiO₂ nanoparticles through covalent bonding.

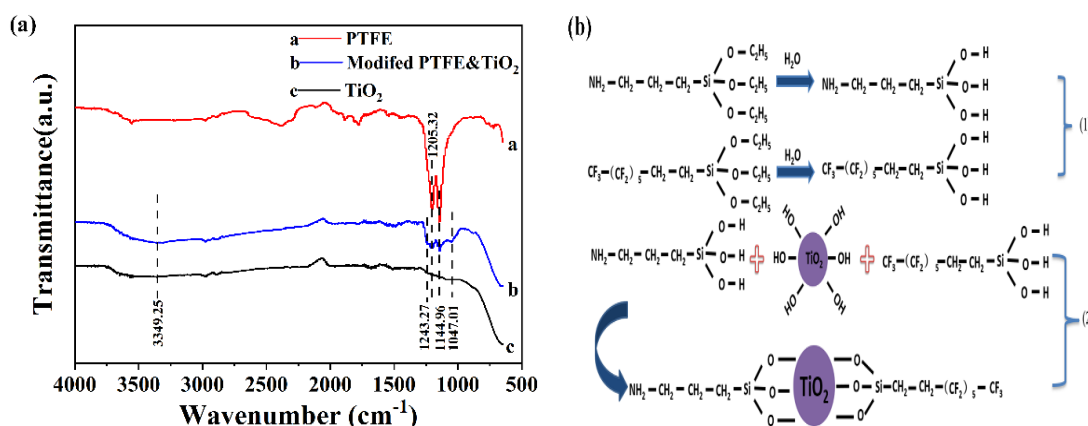


Fig. 5. Fourier transform infrared (FTIR) spectra of PTFE micropowders, TiO₂ nanopowders, and modified hybrid powders(a); possible reaction mechanism diagram for surface modification (b).

3.3. Chemical Stability Testing

Long-term chemical stability is important for superhydrophobic coatings in practical applications. The chemical stability of the coating was tested in 3.5 wt% NaCl solution and varying pH solutions. The hydrophobicity relationship of the samples immersed in varying pH solutions for 12 h is displayed in Fig. 6(a), the hydrophobicity relationship of the samples soaked in NaCl (3.5 wt%) solution for varying times is displayed in Fig. 6(b), the hydrophobicity relationship of the coating immersed in pH 1 solution for varying times is displayed in Fig. 6(c), and the hydrophobicity relationship of the samples soaked in pH 14 solution for varying times is displayed in Figure 6(d).

From Figure 6(a), it is evident that with the gradual increase of alkalinity and acidity, the contact angle is gradually decreasing, the rolling angle is gradually increasing, and the hydrophobicity of the coating has decreased. However, even after immersed in the solution with pH 2 and 13 for 12h, the contact angle can still be greater than 150°, which is still the contact angle required by superhydrophobicity, only the rolling angle changes are larger, which can't satisfy the requirements of superhydrophobicity, which is due to the large amount of acid and alkali ions invading the surface of superhydrophobic coating, which destroys the integrity of the surface of coating. It is still superhydrophobic at pH 5-10, and the contact angles of the samples are all greater than 150°, and the rolling angles are all less than 10°, which indicates that the

samples have better tolerance in alkaline acid. From Figure 6(c) and (d), it is evident that the samples were immersed in an aqueous solution of pH 1 for 32 hours, and the coating contact angle was 143.6° ; in an aqueous solution of pH 14 for 25 hours, the coating contact angle was 137.8° . This indicates that the samples have good properties in acids and bases.

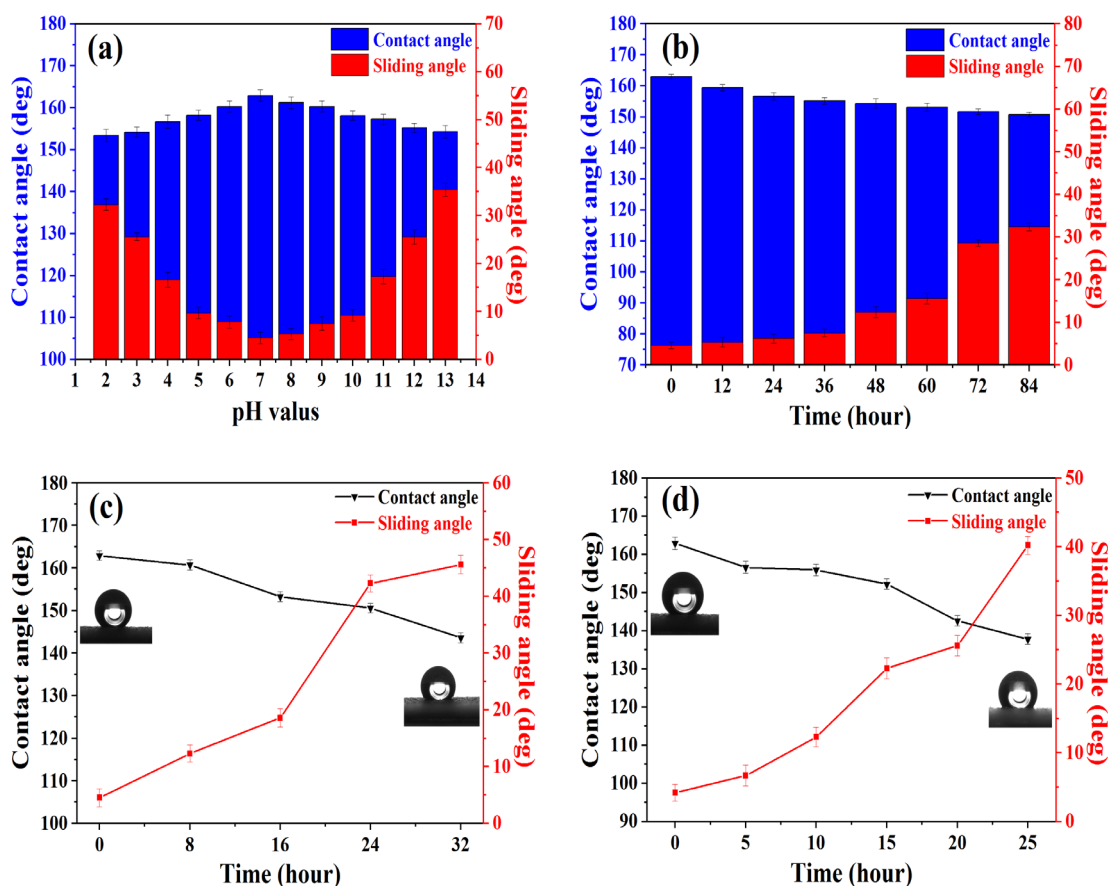


Fig. 6 Changes in wetting of samples soaked in different chemical reagents. (a) The hydrophobicity relationship of the samples immersed in varying pH solutions for 12 h; (b) the hydrophobicity relationship of the samples soaked in NaCl (3.5 wt%) solution for varying times; (c) the hydrophobicity relationship of the coating immersed in pH 1 solution for varying times; (d) the hydrophobicity relationship of the samples soaked in pH 14 solution for varying times.

From Fig. 6(b), it is evident that the contact angle of the sample is 150.7° after being soaked in NaCl (3.5 wt%) corrosive reagent for 84h, which still achieves superhydrophobicity, only that the rolling angle exceeds the superhydrophobicity requirement, this is due to the fact that as time passes, Na^+ and Cl^- begin to erode the superhydrophobic coating's waterproof layer before penetrating its interior and causing coating destruction. Overall the sample has good properties in NaCl (3.5 wt%) reagent.

The cause of the good chemical stability of the coating is due to the large amount of air stored on the surface of the coating to form an air layer, so that the contact area between the corrosive solution and the coating decreases dramatically.

3.4. Adhesion test

The adhesion of the PTFE@TiO₂/EP superhydrophobic coating was evaluated according to the international standard Paint and varnish - Cross-cut test (ISO 2409-2013). It is obvious from Figs. 7(b) and (d) that the coating surface is free from defects, the edges of the cut cross are completely smooth and there is no grid shedding. Referring to the grading of the international criterion experimental results it is evident that the superhydrophobic coating has a bonding force of level 0 (the highest level). This indicates that the samples have high utility and excellent adhesion.

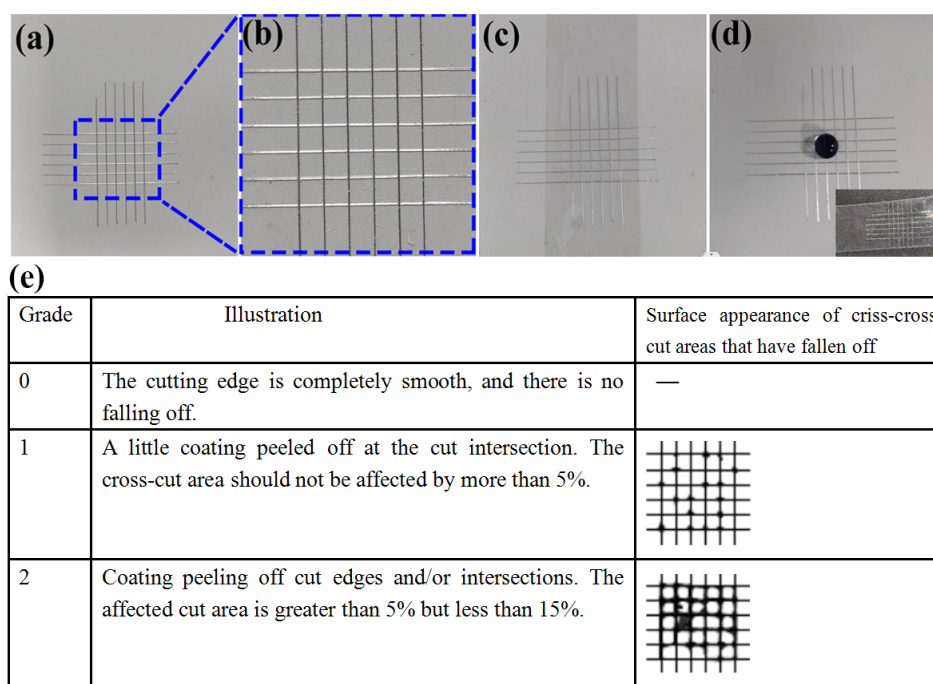


Fig. 7. (a) Adhesion test on samples; (b) is a magnified image of the coated surface; (c) tape is applied to the coated surface; (d) the tape has a tiny amount of powder on it; and (e) is ISO2409-2013.

3.5. Abrasion resistance test

In practice, the coating will inevitably be damaged due to external factors. As illustrated in figure 8 (a), the coating contact angle falls with the increase of the number of abrasion, the sample is still superhydrophobic when the number of abrasion reaches 80 times, with a contact angle of 156.2° and a rolling angle of 9.7°, and after 180 abrasion tests, the hydrophobicity of the sample decreases, and the contact angle is 148.6°, and the sample is still hydrophobic with good hydrophobicity. The reason why the coating can achieve such an effect is mainly due to the micro-nanoparticles and the epoxy resin are cured together, which sticks the stuffed nanoparticles firmly on the outside of the aluminium sheet, which is not easy to be abraded, so that the surface still has good hydrophobicity.

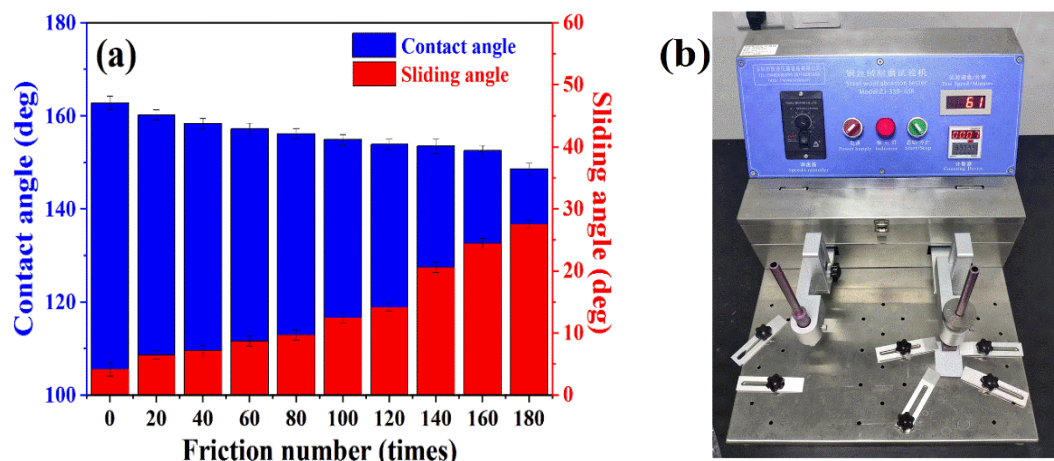


Fig. 8. (a) Effect of wear on the wettability of PTFE@TiO₂/epoxy superhydrophobic coating; (b) Schematic diagram of wear resistance experiment.

3.6. Thermal stability test

The hydrophobicity changes of the PTFE@TiO₂ / epoxy composite superhydrophobic coatings at different temperatures were tested, as displayed in Figure 9. From Figure 9(b), it is evident that when the sample is at 200 °C, the coating changes from white to light yellow; when the coating is at 300 °C, the coating changes from light yellow to brown, which is due to the oxidation reaction of the white PTFE micropowder under the action of high temperature and oxygen, which makes the coating colour change. Although the coating colour changes under high temperature conditions, some basic properties of the coating do not change. As can be seen in Figure 9(a), the contact angle of the coating is greater than 150° and the rolling angle is less than 10° throughout the temperature interval, indicating that the PTFE@TiO₂ / epoxy composite superhydrophobic coatings have good thermal stability.

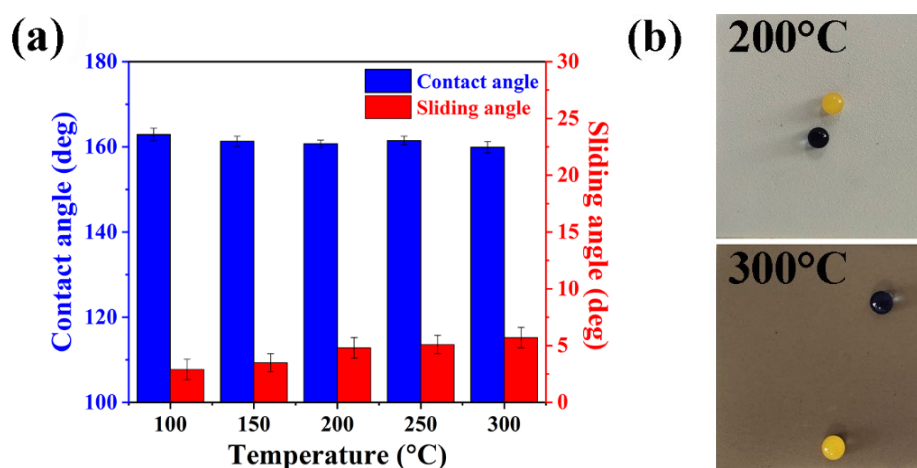


Fig. 9. (a) Change in hydrophobicity of coating at different temperatures; (b) Change in surface of coating at different temperatures.

3.7. Self-cleaning and antifouling performance testing

The sample was tilted at a certain angle, and at the higher end of the sample, the water droplets slowly dripped down from a distance of 1 cm from the sample surface. From Fig. 10 (a1-a3), it can be seen that all kinds of common liquid pollutants dropped on the surface of superhydrophobic coating not only will not be adsorbed, but also will be quickly slid off the surface, which proves that the coating has significant hydrophobicity. From Fig. 10 (b1-b3), it can be seen that when the droplets drop sequentially on the common coating, there are still many dust and water stains remaining on the surface of the ordinary coating; from Fig. 10 (c1-c3), it can be seen that after the superhydrophobic coating of PTFE@TiO₂/epoxy resin is intentionally contaminated by dust, the water droplet rolls down from the surface of the coating, and the dust is taken away by the water droplets all wrapped up. It shows that the PTFE@TiO₂/epoxy resin superhydrophobic coating has good self-cleaning properties.

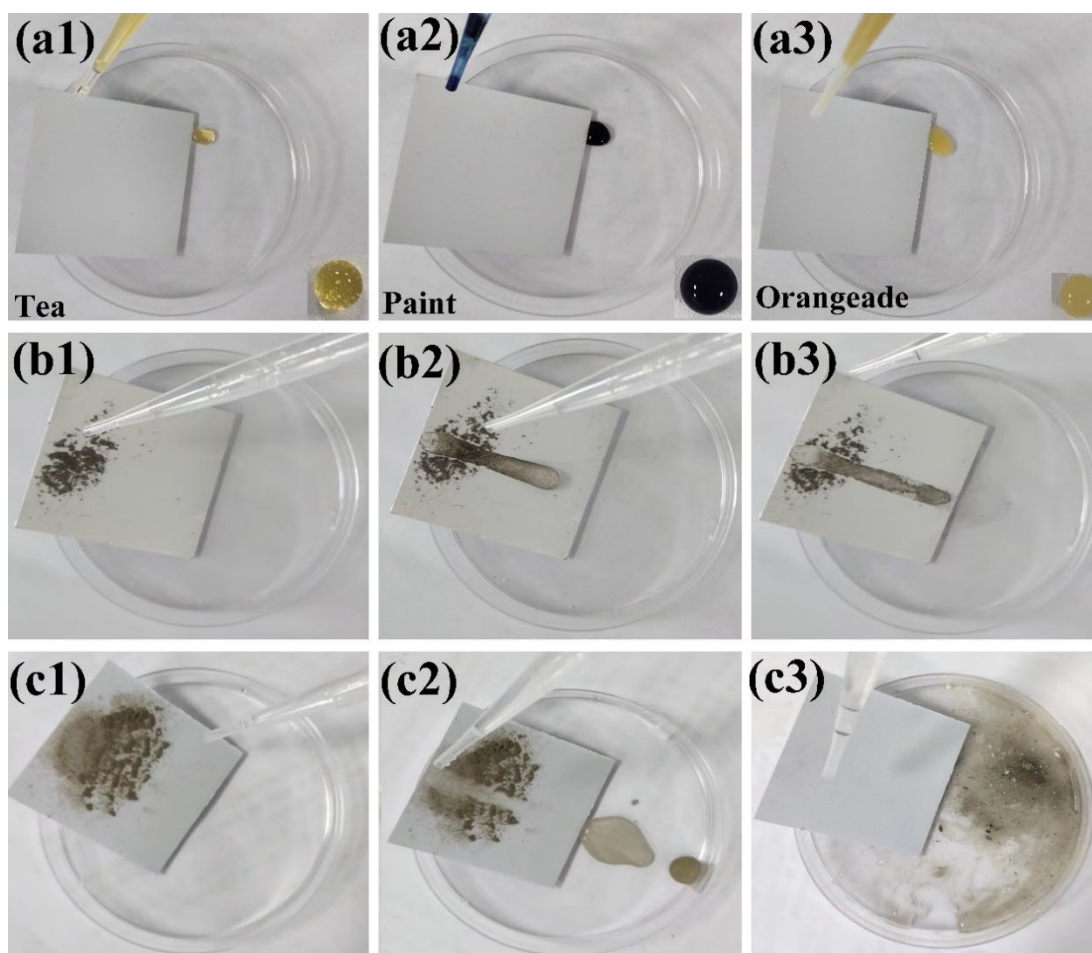


Fig. 10. (a1-a3) Self-cleaning test of PTFE@TiO₂/epoxy superhydrophobic coating under daily liquid; (b1-b3) Self-cleaning test of normal coating contaminated by dust; (c1-c3) Self-cleaning test of PTFE@TiO₂/epoxy superhydrophobic coating contaminated by dust.

In order to test the antifouling performance of the coatings, the antifouling performance of the aluminium sheet, the normal coating, and the PTFE@TiO₂/epoxy superhydrophobic coating were tested using the aqueous solution of methylene blue as a model source of

contamination. As shown in Fig. 11(a1-a3), the surface of the aluminium sheet was contaminated with stained water when it was immersed in the aqueous solution of methylene blue and removed from the sewage. From Fig. 11 (b1-b3), it can be seen that the surface of the common coating is not varying from the surface of the aluminium sheet in terms of its antifouling effect, and neither of them can achieve antifouling; from Fig. 11 (c1-c3), it can be seen that the surface of the PTFE@TiO₂/epoxy superhydrophobic coating is not contaminated and remains clean, which indicates the excellent antifouling performance of the PTFE@TiO₂/epoxy superhydrophobic composite coating. This is due to the fact that the air layer of the coating acts as a barrier, effectively preventing liquids from wetting and contaminating the surface, making it easier to slip off the surface^[52].

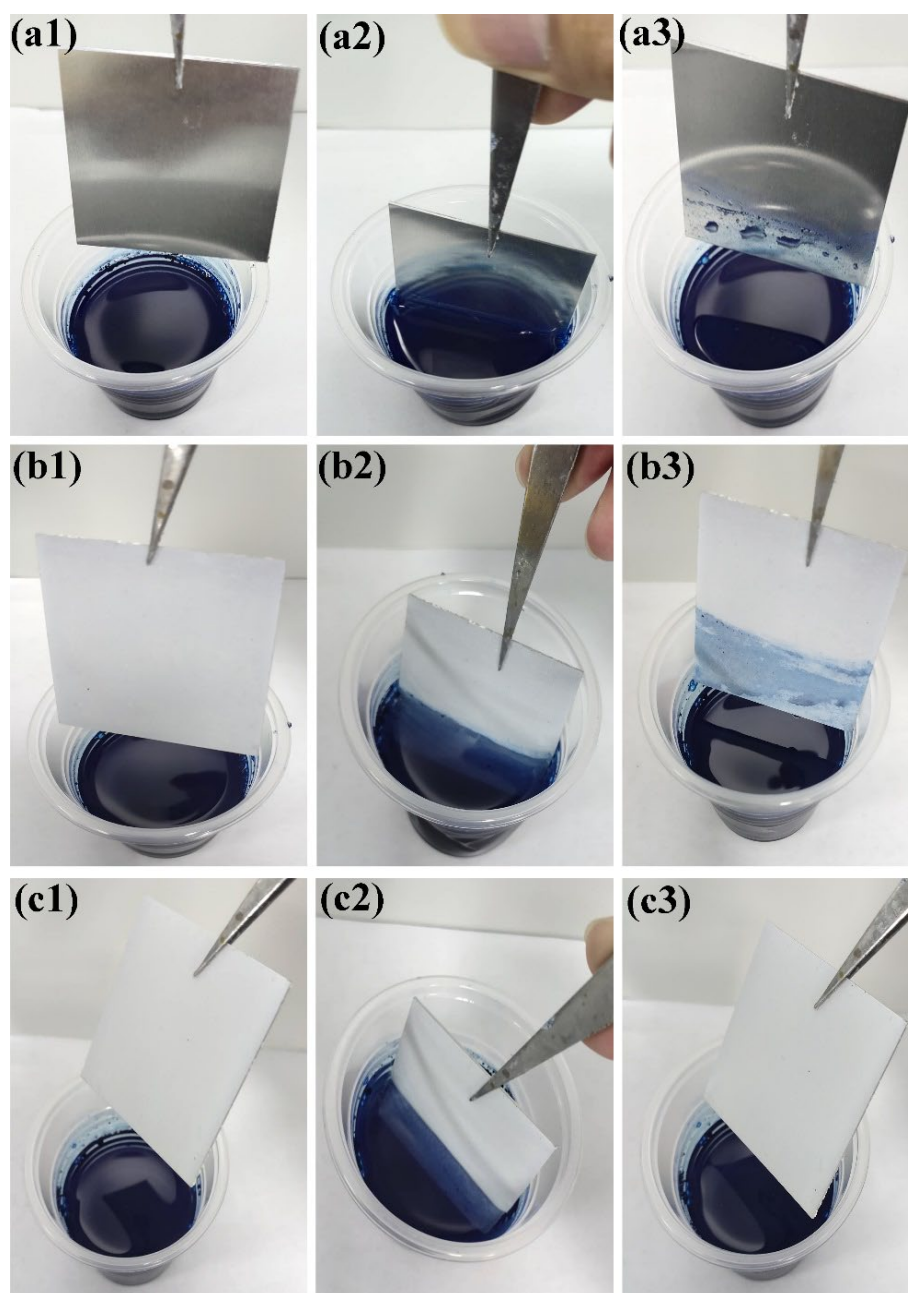


Fig. 11. Antifouling process of untreated aluminium sheets (a1-a3); normal coating (b1-b3) and PTFE@TiO₂/epoxy superhydrophobic coating (c1-c3).

3.8. Antimicrobial performance test

Bacterial adherence in production and life brings many hidden dangers to human beings. We chose *Escherichia coli* bacteria to test the antimicrobial properties of the coating. *Escherichia coli*, often referred to as *E. coli*, is a Gram-negative bacterium that is widely found in nature. The antimicrobial test was carried out using LB nutrient agar medium and the results are shown in Table 1 as well as Figure 12. Figure 12 shows the growth of *E. coli* on solid medium in blank control sample, PTFE coated as well as PTFE@TiO₂/epoxy superhydrophobic coated groups. A large number of *E. coli* appeared on the surface of the nutrient agar plate of the blank control sample (HDPE), while the number of *E. coli* on the surface of the PTFE@TiO₂/epoxy superhydrophobic-coated nutrient agar plate was much less than that of the blank control sample (HDPE). According to the antimicrobial formula $R=(B-A)/B\times 100\%$, the antimicrobial rate of the PTFE coating can be up to 69.5%, and the antimicrobial rate of the PTFE@TiO₂/epoxy superhydrophobic coating can be up to 98.2%. It shows that the PTFE@TiO₂/epoxy superhydrophobic coating has good anti-adhesion effect on bacteria.

Table 1. Antimicrobial performance test results of different samples against *E. coli*.

Sample	Colony count	Antibiosis rate
Blank control(HDPE)	338	-
PTFE coating	103	69.5%
PTFE@ TiO ₂ Superhydrophobic coating	6	98.2%

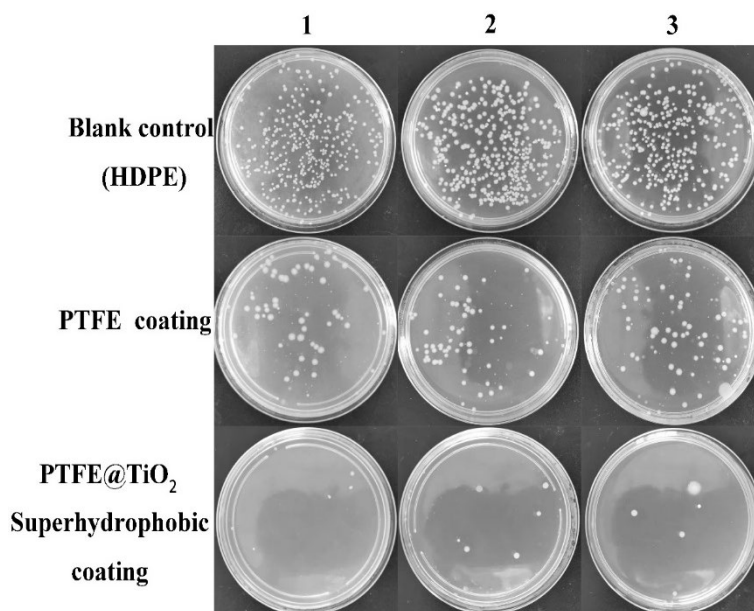


Fig. 12. Antimicrobial test results.

3.9. Antimicrobial mechanism analysis

The antibacterial mechanism of the PTFE@TiO₂/epoxy superhydrophobic coating is illustrated in Fig. 13. The PTFE coating has a slight anti-adhesion effect, which is attributed to the low surface tension of PTFE. The reason why the PTFE@TiO₂/epoxy superhydrophobic coating has a good effect on antimicrobials is that the coating makes it difficult for bacteria to adhere to the superhydrophobic surface by taking advantage of the superhydrophobicity, low adhesion force and low contact area. In addition, the surface of the coating has a large number of nano TiO₂ particles, these particles in the aqueous solution with the bacteria on the membrane surface of the redox reaction, so that the bacteria inactivation, and the surface of the nano TiO₂ has holes will generate electrons, when the more electrons generated by the holes, its electrons can be reacted with the bacteria, the stronger the antibacterial performance. Adequately reduces bacterial adhesion to coated surfaces.



Fig. 13. Schematic of antimicrobial mechanism of PTFE@TiO₂/epoxy superhydrophobic coating.

4. Conclusions

In conclusion, durable PTFE@TiO₂/epoxy superhydrophobic coatings were prepared using a single spraying method. By examining the effects of factors such as the mass ratio between PTFE micropowder and nano-TiO₂ and the mass ratio between POTS and nanoparticles on the wettability of the coatings, it was displayed that the superhydrophobic coatings with the best hydrophobicity, a contact angle of 163.3°, and a rolling angle of 3.2° were prepared with a PTFE micropowder-to-nanoTiO₂ mass ratio of 1:4 and a surface modifier-to-nanoparticle mass ratio of 12%. Moreover, the coating has better wear resistance and adhesion performance, the contact angle of the coating surface is 148.6° after 180 wear experiments, and the bond measurement between the coating and the substrate reaches grade 0 (the highest grade). Meanwhile, the antimicrobial results showed that the prepared superhydrophobic coatings had good antimicrobial properties (antimicrobial rate of 98.2%). This is mainly due to the low contact area and self-cleaning performance of the superhydrophobic surface, combined with the antimicrobial properties of TiO₂ nanoparticles, which sufficiently reduces bacterial adhesion to the coated surface.

Acknowledgements

This work was supported by the National Natural Science Foundation of China (52073127) and the International Science and Technology Cooperation Project of Changzhou Science and Technology Bureau (CZ20230024).

References

- [1] Sahin F, Celik N, Ceylan A, et al., *Chemical Engineering Journal*, 2022, 431; <https://doi.org/10.1016/j.cej.2021.133445>
- [2] Chen L, Duan Y, Cui M, et al., *Sci Total Environ*, 2021, 766: 144469; <https://doi.org/10.1016/j.scitotenv.2020.144469>
- [3] Ali A, Jamil M I, Jiang J, et al., *Journal of Polymer Research*, 2020, 27(4): 85; <https://doi.org/10.1007/s10965-020-02054-z>
- [4] Han X, Wu J, Zhang X, et al., *Journal of Materials Science & Technology*, 2021, 61: 46-62; <https://doi.org/10.1016/j.jmst.2020.07.002>
- [5] Wei T, Qu Y, Zou Y, et al., *Current Opinion in Chemical Engineering*, 2021, 34: 100727; <https://doi.org/10.1016/j.coche.2021.100727>
- [6] Hadzhieva Z, Boccaccini A R., *Current Opinion in Biomedical Engineering*, 2021: 100367; <https://doi.org/10.1016/j.cobme.2021.100367>
- [7] Sharifikolouei E, Najmi Z, Cochis A, et al., *Materials Today Bio*, 2021, 12: 100148; <https://doi.org/10.1016/j.mtbio.2021.100148>
- [8] S. Parani, O.S. Oluwafemi, *Materials Letters*, 281 (2020); <https://doi.org/10.1016/j.matlet.2020.128663>
- [9] C. Cao, F. Wang, M. Lu, *Materials Letters*, 260 (2020); <https://doi.org/10.1016/j.matlet.2019.126956>
- [10] H. Jin, M. Kettunen, A. Laiho, H. Pynnönen, J. Paltakari, A. Marmur, O. Ikkala, R.H.A. Ras, *Langmuir*, 27 (2011) 1930-1934; <https://doi.org/10.1021/la103877r>
- [11] F. Zhang, L. Zhao, H. Chen, S. Xu, D.G. Evans, X. Duan, *Angewandte Chemie*, 120 (2008) 2500-2503; <https://doi.org/10.1002/ange.200704694>
- [12] Z. Li, C. Li, J. Ou, X. Fang, M. Cong, C. Wang, F. Mao, T. Mao, A. Amirfazli, *RSC Adv*, 11 (2021) 21862-21869; <https://doi.org/10.1039/D1RA03140F>
- [13] Y. Lu, S. Sathasivam, J. Song, C.R. Crick, C.J. Carmalt, I.P. Parkin, *Science*, 347 (2015) 1132-1135; <https://doi.org/10.1126/science.aaa0946>
- [14] L. Wang, Q. Gong, S. Zhan, L. Jiang, Y. Zheng, *Adv Mater*, 28 (2016) 7729-7735; <https://doi.org/10.1002/adma.201602480>
- [15] H. Li, S. Yu, *Appl. Surf. Sci.*, 420 (2017), 336-345; <https://doi.org/10.1016/j.apsusc.2017.05.131>
- [16] T. Zhu, S. Li, J. Huang, M. Mihailiasa, Y. Lai, *Mater. Des.*, 134 (2017), 342-351; <https://doi.org/10.1016/j.matdes.2017.08.071>
- [17] C. Xia, Y. Li, T. Fei, W. Gong, *Chem. Eng. J.*, 345 (2018), 648-658; <https://doi.org/10.1016/j.cej.2018.01.079>

- [18] J. Li, Z. Zhao, D. Li, H. Tian, F. Zha, H. Feng, L. Guo, *Nanoscale*, 9 (2017), 13610-13617; <https://doi.org/10.1039/C7NR04448H>
- [19] Y. Huang, Y. Shan, S. Liang, X. Zhao, G. Jiang, C. Hu, J. Yang, L. Liu, *J. Mater. Chem. A*, 6 (2018), 17156-17163; <https://doi.org/10.1039/C8TA02893A>
- [20] M. Cheng, S. Zhang, H. Dong, S. Han, H. Wei, F. Shi, *ACS Appl. Mater. Interfaces*, 7 (2015), 4275-4282; <https://doi.org/10.1021/am5085012>
- [21] H. Zhang, L. Yin, X. Liu, R. Weng, Y. Wang, Z. Wu, *Appl. Surf. Sci.*, 380 (2016), 178-184; <https://doi.org/10.1016/j.apsusc.2016.01.208>
- [22] Z.Y. Xue, C.Q. Li, G.Q. Xu, F.F. Mao, T.C. Mao, A. Amirfazli, *Digest Journal of Nanomaterials and Biostructures*, 18 (2023) 639-656; <https://doi.org/10.15251/DJNB.2023.182.639>
- [23] Jin H, Tian L, Bing W, et al., *Progress in Materials Science*, 2022, 124: 100889; <https://doi.org/10.1016/j.pmatsci.2021.100889>
- [24] He Z, Lan X, Hu Q, et al., *Progress in Organic Coatings*, 2021, 157: 106285; <https://doi.org/10.1016/j.porgcoat.2021.106285>
- [25] T. Zhu, S. Li, J. Huang, M. Mihailiasa, Y. Lai, *Materials & Design*, 134 (2017) 342-351; <https://doi.org/10.1016/j.matdes.2017.08.071>
- [26] Khaleghi H, Eshaghi A., *Surfaces and Interfaces*, 2020, 20: 100559; <https://doi.org/10.1016/j.surfin.2020.100559>
- [27] Zhou H , Wang H , Niu H , et al., *Advanced Materials*, 2012, 24(18):2409-2412; <https://doi.org/10.1002/adma.201200184>
- [28] Lin, Feng, Zhongyi, et al., *Angewandte Chemie International Edition*, 2004; <https://doi.org/10.1002/ange.200353381>
- [29] X.Kong, C.Zhu, J.Lv, et al., *Progress in Organic Coatings*, 138; <https://doi.org/10.1016/j.porgcoat.2019.105342>
- [30] Guang,Xi, Zhang, et al., *Chemical Engineering Journal*, 2019; <https://doi.org/10.1016/j.cej.2019.04.040>
- [31] C.Li, Y.Sun, M.Cheng, et al., *The Chemical Engineering Journal*, 2017:S1385894717316649; <https://doi.org/10.1016/j.cej.2017.09.165>
- [32] X.Wu, Q.Fu, D.Kumar, et al., *Materials & Design*, 2016, 89(JAN.):1302-1309; <https://doi.org/10.1016/j.matdes.2015.10.053>
- [33] Z.Jiang, S.Fang, C.Wang, et al., *Applied Surface Science*, 2016, 390:993-1001; <https://doi.org/10.1016/j.apsusc.2016.08.152>
- [34] J.Mao, M.Ge, J.Huang, et al., *Journal of Materials Chemistry A*, 2017, 5(23):11873-11881; <https://doi.org/10.1039/C7TA01343D>
- [35] K.Hosseinzadeh, D.D.Ganji, F.Ommi, *Journal of Molecular Liquids*, 2020, 315:113748; <https://doi.org/10.1016/j.molliq.2020.113748>
- [36] Wang, Jinfeng, Peng, *Journal of Materials Chemistry A Materials for Energy @ Sustainability*, 2016; <https://doi.org/10.1039/C6TA01082B>
- [37] J.Wu, X.Li, Y.Wu, et al., *Applied Surface Science*, 2017, 422; <https://doi.org/10.1016/j.apsusc.2017.06.076>
- [38] M.Spasoava, N.Manolova, N.Markova, et al., *Applied Surface Science*, 2016,

363(feb.15):363-371; <https://doi.org/10.1016/j.apsusc.2015.12.049>

[39] W.Ban, S.Kwon, J.Nam, et al., Thin Solid Films, 2017, 641(nov.1):47-52;

<https://doi.org/10.1016/j.tsf.2017.02.007>

[40] P.Tao, W.Shang, C.Song, et al., Advanced Materials, 2015.

[41] B.F. Bukit, E. Frida, S. Humaidi, P. Sinuhaji, South African Journal of Chemical Engineering,

41 (2022) 105-110; <https://doi.org/10.1016/j.sajce.2022.05.007>

[42] S. Mallakpour, N. Mohammadi, Carbohydr Polym, 285 (2022) 119226;

<https://doi.org/10.1016/j.carbpol.2022.119226>

[43] A.O. Özdemir, B. Caglar, O. Çubuk, F. Coldur, M. Kuzucu, E.K. Guner, B. Doğan, S. Caglar, K.V. Özdokur, Materials Chemistry and Physics, 287 (2022);

<https://doi.org/10.1016/j.matchemphys.2022.126342>

[44] Z. Luo, Z. Zhang, W. Wang, W. Liu, Q. Xue, Materials Chemistry and Physics, 119 (2010)

40-47; <https://doi.org/10.1016/j.matchemphys.2009.07.039>

[45] Y. Ohko, Y. Utsumi, C. Niwa, T. Tatsuma, K. Kobayakawa, Y. Satoh, Y. Kubota, A. Fujishima, J. Biomed. Mater. Res. 58 (2001)97-101;

[https://doi.org/10.1002/1097-4636\(2001\)58:1<97::AID-JBM140>3.0.CO;2-8](https://doi.org/10.1002/1097-4636(2001)58:1<97::AID-JBM140>3.0.CO;2-8)

[46] Q. Zhao, C. Liu, X. Su, S. Zhang, W. Song, S. Wang, G. Ning, J. Ye, Y. Lin, W. Gong, Appl.

Surf.Sci. 274 (2013) 101-104; <https://doi.org/10.1016/j.apsusc.2013.02.112>

[47] C. Li, Z. Cao, C. Xie, Z. Li, X. Fang, J. Ou, M. Xue, F. Wang, S. Lei, W. Li, Journal of

Applied Polymer Science, 136 (2019); <https://doi.org/10.1002/app.47762>

[48] S. Mallakpoura, V. Shahangia, Designed Monomers and Polymers, 15 (2012) 329-344;

<https://doi.org/10.1163/156855511X615713>

[49] Q. Li, Z. Guo, Nanoscale, 11 (2019) 18338-18346; <https://doi.org/10.1039/C9NR07435J>

[50] H. Liu, W. Geng, C.-J. Jin, S.-M. Wu, Y. Lu, J. Hu, H.-Z. Yu, G.-G. Chang, T. Zhao, Y. Wan, Z.-Q. Luo, G. Tian, X.-Y. Yang, Chemical Physics Letters, 730 (2019) 594-599;

<https://doi.org/10.1016/j.cplett.2019.06.001>

[51] J.D. Brassard, D.K. Sarkar, J. Perron, ACS Appl Mater Interfaces, 3 (2011) 3583-3588;

<https://doi.org/10.1021/am2007917>

[52] X. Kong, J. Zhang, Q. Xuan, J. Lu, J. Feng, Langmuir 34 (28) (2018) 8294-8301;

<https://doi.org/10.1021/acs.langmuir.8b01423>